RSC Advances

Influence of draw ratios on the structure and properties of PEDOT-PSS/PAN composite conductive fibers

Journal:	*RSC Advances*
Manuscript ID:	RA-ART-06-2014-005952.R1
Article Type:	Paper
Date Submitted by the Author:	07-Aug-2014

Complete List of Authors:	Li, Xin; Beijing Institute of Fashion Technology, School of Materials Science & Engineering Liu, Yin; Beijing Institute of Fashion Technology, School of Materials Science & Engineering shi, zheng; Beijing Institute of Fashion Technology, School of Materials Science & Engineering Li, cong; Beijing Institute of Fashion Technology, School of Materials Science & Engineering Chen, Guangming; Institute of Chemistry, Chinese Academy of Sciences,

Cite this: DOI: 10.1039/c0xx00000x

www.rsc.org/xxxxxx

ARTICLE TYPE

Influence of draw ratios on the structure and properties of PEDOT-PSS/PAN composite conductive fibers

Xin Li[a], Yin Liu[a], Zhenghao Shi[a], Congju Li[a]*and Guangming Chen[b]

Received (in XXX, XXX) Xth XXXXXXXXX 20XX, Accepted Xth XXXXXXXXX 20XX

DOI: 10.1039/b000000x

The composite conductive fibers, based on poly(3,4-ethylenedioxythiophene)-polystyrene sulfonic acid (PEDOT-PSS) solution blended with polyacrylonitrile (PAN), were obtained *via* wet spinning. The influence of draw ratios on the morphology, structure, thermal degradation, electrical conductivity, and mechanical properties of the resulted fibers was investigated by SEM, FTIR, XRD, TG, the four-electrode measuring method and electronic single fiber tensile strength tester. The results revealed that the PEDOT-PSS/PAN composite conductive fibers' crystallization, electrical conductivity and mechanical properties were all improved with the increase of draw ratio. The thermal stability of the fibers was almost independent of draw ratios, and only decreased slightly with draw ratio. Besides, when the draw ratio was 6, the conductivity of the PEDOT-PSS/PAN fibers was 5.0 S/cm, ten times of the conductivity when the draw ratio was 2.

1. Introduction

Conductive fibers based on conducting polymers can not only be used to static elimination, detecting and transmitting electrical signals[1-4], but also keep the unique smart sensing features of conducting polymers such as electrochromism and electroluminescence etc., thus having a great application potential in many fields including novel flexible display device, smart window, electronic paper, information storage device, sensor and military camouflage[5-8]. Among the conducting polymers, poly(3,4-ethylenedioxythiophene) doped with poly(4-styrenesulfonate) (PEDOT-PSS), one of the most commercially successful conductive polymers, has attracted wide attention because of its excellent characteristics in its conductive state[9-12]. For example, it has superior electrochemical and thermal stabilities, high optical transparency, high conductivity and easy to be processed, which make it a technologically important material with various potential applications for electronics, especially for organic or plastic electronic and optical devices[13-16]. Wet-spinning is now a widely-used technology to prepare conductive fibers based on conducting polymers. At present, conductive polypyrrole fibers[17], polyaniline composite fibers[18] and pure PEDOT-PSS fibers[19] were all successfully prepared by wet spinning. The pure PEDOT-PSS fibers *via* wet-spinning by Okuzaki et al. have a conductivity of 10^{-1} S/cm with the Young's modulus of 1.1±0.3 GPa, tensile strength of 17.2±5.1 MPa, and elongation at break of 4.3±2.3%[19]. However, confined by its viscosity, it was difficult to spin the pure PEDOT-PSS solution into continuous longer fibers.

In this work, to explore a simple, safe, and industrially viable technique for spinning PEDOT-PSS, self-made PEDOT-PSS solution was blended with polyacrylonitrile (PAN). Then, the traditional wet spinning process was preceded and finally the PEDOT-PSS/PAN composite conductive fibers with excellent electrical conductivity and good mechanical performance were obtained. In addition, the influence of draw ratio on the morphology, structure, thermal degradation, conductivity, and mechanical properties was studied.

2. Experimental

2.1 Materials

3,4-ethylenedioxythiophene (EDOT, ≥99.5%) was provided by Suzhou Yacoo chemical reagent corporation. Polystyrene sulfonic acid (PSS, CP, Mw=100000) was produced by Shanghai Jiachen chemical Co., Ltd. Ferric trichloride ($FeCl_3$, AR) was purchased from Xi Long chemical Co., LTD. Sodium persulfate ($Na_2S_2O_8$, AR) was provided by Tianjin Damao Chemical Reagent Factory. Polyacrylonitrile (PAN, Mw=50000±5000) was

purchased from China's Oil Daqing Lianhua Company. Sodium thiocyanate (NaSCN) was purchased from Beijing Chemical Works. The water used in the synthesis was distilled water. All reagents were used as received without further purification.

2.2 Preparation of PEDOT-PSS

PEDOT-PSS dispersions were prepared by chemical oxidative polymerization. Firstly, 0.15 g of EDOT was blended with 0.41g PSS. Secondly, 7 mL water was added into the mixture and stirred for 15 min, then added the solution of 0.38g $Na_2S_2O_8$ dissolving in 6 mL water into the mixture. Thirdly, 0.45 mL $FeCl_3$ solution (1 mol/L) was diluted with 7mL water and then was added dropwisely to the previous solution. Lastly, the mixture was stirred for 24h at room temperature. The obtained mixture was called PEDOT-PSS and used in the following experiment. The conductivity of the resulted PEDOT-PSS is measured as 1.52S/cm.

2.3 Preparation of the Spinning Solution

20g NaSCN were added into 20mL PEDOT-PSS solution. Then, 6.0g PAN powder was added into the PEDOT-PSS and NaSCN mixtures in order to make into 13% PAN spin dope which included 1.83wt% PEDOT-PSS. Finally, the dissolved solutions were placed in a vacuum drying oven at 45℃ for 2 days to degas. The dope obtained in this way was called PEDOT-PSS/PAN mixture, and the conductivity of the resulted PEDOT-PSS/PAN is measured as 0.64S/cm.

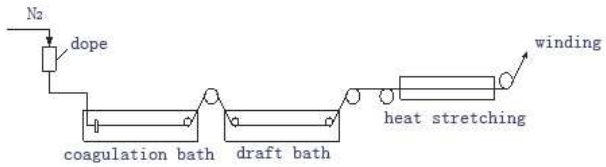

Fig. 1. Schematic diagram of the wet-spinning process

2.4 Preparation of the Composite Conductive Fibers

The PEDOT-PSS/PAN fibers were fabricated with a wet spinning technique with a multihole spinneret (18 holes, Φ=0.2mm). Fig. 1 gives the schematic diagram of the wet-spinning process used in this study. Nitrogen gas was used to provide the required pressure extruding the dope from the reservoir into the spinneret. The coagulation bath was filled up with NaSCN solution with a concentration of 10wt%. The temperature of the coagulation bath was maintained at 0~5□ and controlled by ice. The draft bath was filled with NaSCN solution with a concentration of 4 wt%. The temperature of the draft bath was maintained at 50□ controlled by a potential transformer. The resulting microfibers were then placed on a hot plate (160□) and undergone continuously winding.

2.5 Characterization

The scanning electron microscope (JSM-6360LV, the Japanese electronics company, Japan) was used to collect electron micrographs of the PEDOT-PSS/PAN fibers. The imaging conditions were 10.0 kV and work distance=29mm. The structure of the fibers was analyzed by a Nexus 670 Fourier transform infrared (FTIR, Nicolet company, America) spectroscope. X-ray diffraction (XRD) patterns of powder samples were recorded with Cu Kα radiation (λ=1.5406 Å) at 40 kV and 50 mA with a Rigaku wide-angle goniometer, Japan RIGAKU company, Japan. The data were collected in the range $6°<2\theta<36°$. The thermostability was observed by a TG6300 (SII company, Japan) instrument operating at a heating rate of 10℃/min under a nitrogen atmosphere. The temperature range was 20-800 ℃. The tensile strength and breaking elongation values of fibers were measured by using YG004N electronic single fiber tensile strength tester, Nantong Dahong experimental instrument company, China. The jaw gap was 20cm and the extension rate was kept constant at 10cm/min.

The electrical conductivities of the samples were measured by four-probe conductivity meter (Keithley 6221+2182A, Keithley Instruments Inc., America) at room temperature and humidity of 40%R.H. Three different samples are used for measurement and the final results are their average value. The diameters of the fibers were measured *via* scanning electron microscopy (SEM) images. The conductivities were calculated by the following formula:

$$\delta = IL/VS \quad (1)$$

where δ is the conductivity (S/cm), I is the constant current through the two outer electrodes, V is the variational potential through the two inner electrodes, L is the distance of the two inner electrodes, and S is the area of the fiber section.

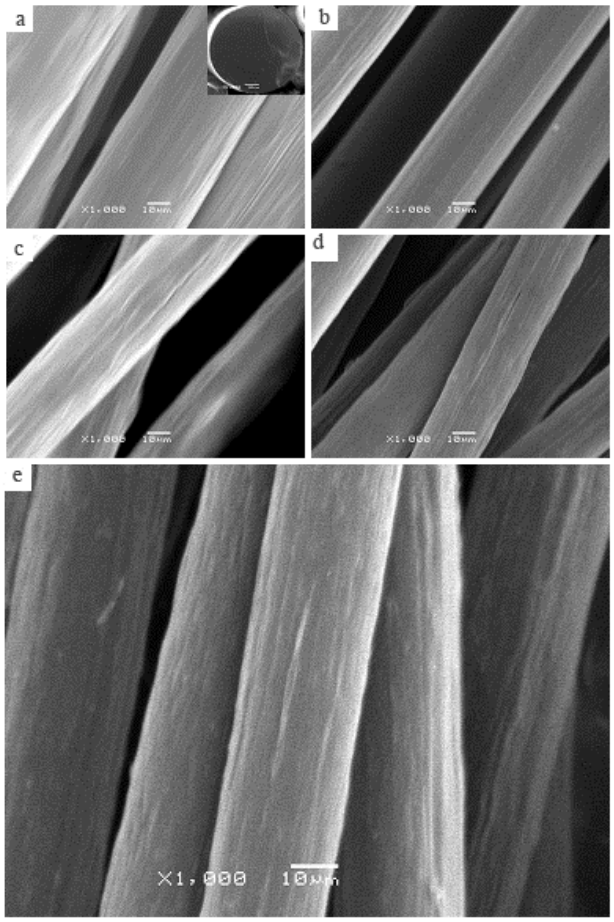

Fig. 2. The SEM images of PEDOT-PSS/PAN composite conductive fibers with different draw ratios:

(a) 2; (b) 3; (c) 4; (d) 5; (e) 6.

3. Results and Discussion

3.1 Morphology

The SEM images of PEDOT-PSS/PAN composite conductive fibers on different draw ratios are displayed in Fig. 2. From Fig. 2, it can be seen that the diameter of all the fibers is in the range of 25~50μm. Moreover, with the increase of the draw ratio, the diameter of the fiber decreased. When the draw ratio is 2, the diameter of the PEDOT-PSS/PAN composite conductive fibers is about 50 μm, however, when the draw ratio increases to 6, the diameter of the fiber decreases to 25 μm. From the insert SEM picture (Fig. 2a), it is clear that the intersecting surfaces of PEDOT-PSS/PAN composite conductive fiber are circular and homogeneous without any holes and cracks. In our previous work[20], we have found that the intersecting surfaces of PEDOT-PSS/PAN composite conductive fibers with different PEDOT-PSS content and pure PAN fibers are all circular, and the surface of the pure PAN fibers is smooth without any microfibril structure. However, in this study, it is clear that the surfaces of the fibers PEDOT-PSS/PAN composite conductive fibers (Fig.2) have much microfibril structure parallel with the axial direction of thefiber, indicating the condcutive material is oriented along the drawing direction during the drawing process.

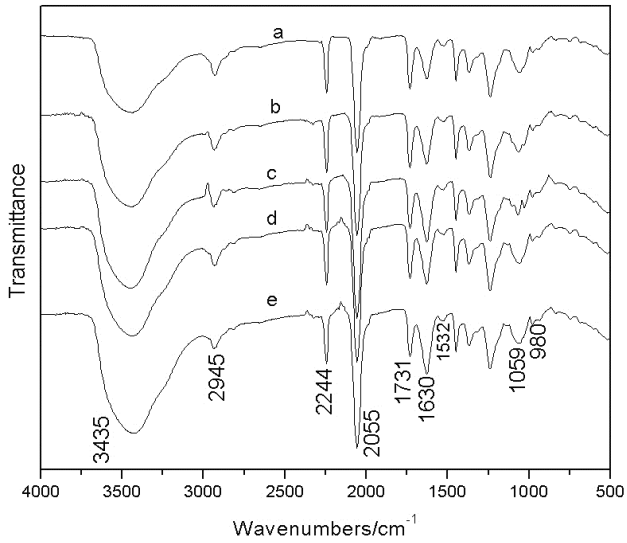

Fig. 3. FTIR spectra of PEDOT-PSS/PAN composite conductive fibers with different draw ratios:

(a) 2; (b) 3; (c) 4; (d) 5; (e) 6.

3.2 FTIR Analysis

The FTIR spectra of PEDOT-PSS/PAN composite conductive fibers on different draw ratios are given in Fig. 3. It can be seen from Fig. 3 that all the spectra of PEDOT-PSS/PAN composite fibers share similar profile. FTIR spectra of PEDOT-PSS/PAN composite fibers show several characteristic bands, such as those at 2244 cm^{-1} for -CN stretching and 1731 cm^{-1} for -CO stretching[21]. The absorption band at 2055 cm^{-1} is attributed to -SCN. The weak absorption band at 1532 cm^{-1} and 980 cm^{-1} are assigned to the benzenoid rings of PSS and -C-S-C- deformation vibration of PEDOT-PSS[22], respectively. It is proved that the PEDOT-PSS is present in PEDOT-PSS/PAN fibers. Besides, the intensity of the PEDOT-PSS/PAN composite conductive fibers' absorption peak at 3435 cm^{-1} assigned as intermolecular N-H stretching vibration of PAN and the sharp peak at 2055 are increased with the draw ratio increase, which is because the orientation degrees of the macromolecular chain along the axis of the fibers are increased so that the intermolecular forces are gradually increased.

3.3 XRD Analysis

Fig. 4 displays the XRD diffraction patterns of the composite fibers obtained at different draw ratios. From Fig. 4, it can be known that the XRD patterns of the composite conductive fibers with different draw ratios are all similar. Obviously, the strongest diffraction peak from the PEDOT-PSS/PAN composite conductive fiber occurs at around 2θ=17.6° in Fig. 4, which can

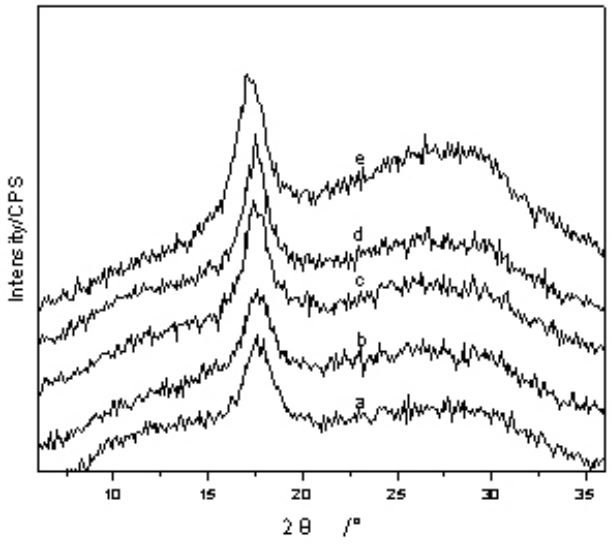

Fig. 4. XRD diffraction patterns of PEDOT-PSS/PAN composite conductive fibers with different draw ratios:

(a) 2; (b) 3; (c) 4;(d) 5; (e) 6.

be indexed to the (100) plane of a hexagonal structure[22].The broad diffraction peaks centered at 27.5° indicated that the crystallization of the PEDOT-PSS/PAN composite conductive fibers was in the amorphous phase. Moreover, with the increase of the draw ratios, the peak of the (100) plane appeared gradually blue shift from 17.6° to 17.1°. Furthermore, the increased strength of the diffraction peaks with the draw ratio increase indicates the improved crystallization of the PEDOT-PSS/PAN composite fibers, which may be due to the increasing of the orientation degrees of the macromolecular chain along the axis of the fibers leading to the more orderly molecular structure. As a result, the crystallization is improved.

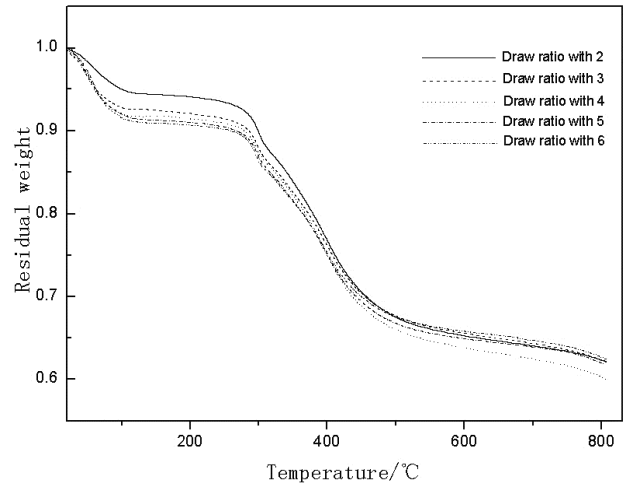

Fig. 5. TG curves of the PEDOT-PSS/PAN composite conductive fibers with different draw ratios:

(a) 2; (b) 3; (c) 4; (d) 5; (e) 6.

3.4 Thermal Stability

Thermal stability of the PEDOT-PSS/PAN composite fibers is studied by TG, which is an important method to detect the degradation behavior of the fibers. As shown in Fig. 5, the thermograms are similar to each other for all PEDOT-PSS/PAN composite fibers with different draw ratios. It is clear that the loss of conductive fiber is mainly divided into three stages. The first weight loss of 5-9% at 20~110□ is attributed to the elimination of moisture adsorbed[23], and the second one at 280~500 □ represents the degradation of the PAN molecular chains[24]. The third stage is the constant weight stage since 500□. Besides, the final amount of residual carbon was from 58 to 63%. From Fig. 5, it can be seen that the thermal stability of the PEDOT-PSS/PAN composite conductive fibers is decreased with the draw ratio increase.

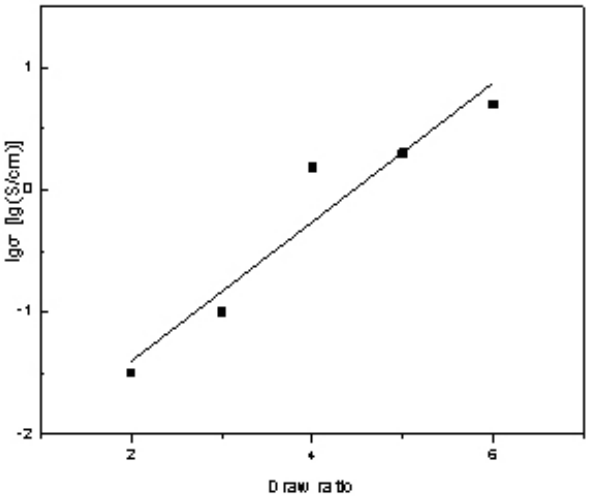

Fig. 6. The relation of the draw ratio of PEDOT-PSS/PAN fibers and the conductivity

of the PEDOT-PSS/PAN composite fibers.

3.5 Electrical Conductivity

Fig. 6 gives the relationship between the draw ratio and the electrical conductivity of the PEDOT-PSS/PAN composite conductive fibers. From Fig. 6, it can be seen that the fibers' conductivity multiplies with the draw ratios increase. When the draw ratio is 6, the conductivity of the fiber is 5.0 S/cm, which is ten times of the conductivity when the draw ratio is 2. This conductivity is much higher than that of the pure PEDOT-PSS fiber (0.1 S/cm) prepared by Okuzaki and Ishihara[19], although the content of PEDOT-PSS in the whole composite fiber is only 1.83%. The reason for this phenomenon may comes from three aspects: firstly, although the content of PEDOT-PSS is low, a kind of consecutive phase in the solid fiber has been formed,

which is an effective conductive path of the electron conduction in the solid fiber; secondly, the high draw ratio results in highly orientate of the PEDOT-PSS molecular, forming a kind of fully straight molecular conformation which is the more effective conductive channel in the PAN matrix[20]; thirdly, with the increase of the draw ratio, the quantity of the fibril structure in the fibers also increases, which makes the amounts of the conductive channel increase. This condition is similar with that we have found in the PEDOT-PSS/PVA composite conductive fibers[25].

3.6 Mechanical Performance

The drawing strength is the most important index of fiber spinnability, and it has a close relationship with the process performance. Through testing the stress-strain curve of the PEDOT–PSS/PAN composite fibers with different draw ratios, we found that for all of the samples, there existed yield points, which belonged to strong and tough materials[26]. The tensile test results are tabulated in Table 1. As shown in Table 1, we can know that the breaking strength and initial modulus of pure PAN fibers and composite conductive fibers are all increased with the draw ratio increase, while the elongation at break decrease with the draw ratio increase. The parameters of the pure PAN fibers are all higher than the PEDOT–PSS/PAN composite fibers at the same draw ratio. When the draw ratio is 2, the breaking strength of PEDOT–PSS/PAN composite fiber is 0.12 cN/dtex, the elongation at break is 56.01% and the initial modulus is 0.55 cN/dtex. When the draw ratio is 6, the breaking strength, elongation at break and initial modulus of PEDOT–PSS/PAN composite fibers are 0.73 cN/dtex, 33.23% and 3.97 cN/dtex, respectively, which are over 6 times, 59% and 7.2 times compared with that of parameters when the draw ratio is 2 respectively. Therefore, it is concluded that the PEDOT-PSS/PAN composite conductive fiber's mechanical performance is getting better and better as the draw ratio increased. If make further improvement on the draw ratio, the mechanical performance will be better. This may be one effective way to improve the mechanical performance and conductivity of the PEDOT-PSS/PAN composite conductive fiber.

Table 1. The mechanical properties of pure PAN and PEDOT-PSS/PAN fibers with different draw ratios

Draw ratio	Breaking strength /(cN/dtex)		Elongation at break /(%)		Initial modulus /(cN/dtex)	
	PAN	PEDOT-PSS/PAN	PAN	PEDOT-PSS/PAN	PAN	PEDOT-PSS/PAN
2	0.38	0.12	64.32	56.01	3.37	0.55
3	0.49	0.23	55.24	47.89	4.21	1.89
4	0.60	0.36	49.91	36.73	5.06	3.32
5	0.75	0.60	42.09	35.19	5.54	3.63
6	0.87	0.73	38.42	33.23	5.95	3.97

4. Conclusions

PEDOT-PSS/PAN composite conductive fibers were successfully prepared by wet spinning process, which is a kind of simple, safe, and industrially viable technique. The crystallization and mechanical properties of the obtained PEDOT-PSS/PAN conductive composite fibers were enhanced with the increase of draw ratio. The thermal stability of the fibers with different draw ratios was similar with each other and a little lower with the draw ratio increase. The fiber with 1.83 wt% PEDOT-PSS showed a conductivity as high as 5.0 S/cm when the draw ratio was 6.

Acknowledgements

The authors gratefully acknowledge the financial support of Scientific and Technology Key Project of Beijing Educational Committee (No. KZ201410012017), and Training Program of the Scientific Research Promotion Plan of Beijing Institute of Fashion Technology (No. 2014AL-04), and College Student Research Program (No. 37). The financial support by National Natural Science Foundation of China (No. 51343005) is also acknowledged.

Notes and references

[a] *Beijing Key Laboratory of Clothing Materials R&D and Assessment, School of Materials Science & Engineering, Beijing Institute of Fashion Technology, Beijing 100029, PR China. E-mail: clylx@bift.edu.cn*

[b] *Beijing National Laboratory for Molecular Sciences (BNLMS), Institute of Chemistry, Chinese Academy of Sciences, Beijing 100190, P. R. China. E-mail: chengm@iccas.ac.cn*

1 A. Ramanavičius, A. Ramanavičienė and A. Malinauskas, *Electrochimica Acta,* 2006, **51**, 6025.

2 M. Gerard, A. Chaubey and B.D. Malhotra, *Biosensors and Bioelectronics,* 2002, **17**, 345.

3 M.X. Wan, *Adv. Mater.*, 2008, **20**, 2926.

4 K. Bohwon, K.Vladan, D. Eric, D. Claude and V. Pierre, *Synth. Met.*, 2004, **146**, 167.

5 X. Li, G. L. Zhao, J. Qian and Zh. Y. Fu, *Chemical Journal of Chinese Universities*. 2009, **30**, 1052.

6 S. Beaupré, J. Dumas and M. Leclerc, *Chem. Mater.*, 2006, **18**, 4011.

7 X. Li, J. Qian and Zh.Y. Fu. *Journal of Beijing Institute of Fashion Technology*, 2009**, 29**, 12.

8 X. Li, X. N. Li, Zh. Y. Fu, Zh. K.Yang and L. Zhao, *Journal of Beijing Institute of Fashion Technology*, 2008, **28**, 58.

9 T. Lindfors, Zh. A. Boeva and R. M. Latonen, *RSC Adv.*, 2014, **4**, 25279.

10 N. Kim, S. Kee, S. Ho Lee, B. Hoon Lee, Y. H. Kahng, Y. R. Jo, B. J. Kim and K. Lee, *Adv. Mater.*, 2013,**3**, 22065.

11 H. J. Song, C. C. Liu, J. K. Xu, Q. L. Jiang and H. Shi, *RSC Adv.*, 2013, **3**, 22065.

12 K. Xu, G. Chen, D. Qiu, J. Mater. Chem. A, 2013, 1, 12395.

13 T. Y. Chiang, M. Ch. Huang and Ch. H. Tsai, *RSC Adv*., 2014, **4**, 21201.

14 R. Sydam and D. M. Deepa, *ChemPlusChem*, 2012, 77, 778.

15 Z. G. Tang, Q. M. Liu, I. Khatri, R. Ishikawa, K. J. Ueno and H. Shirai, *Physica Status Solidi (c)*, 2012, **9**, 2075.

16 I. Schwendeman, C.L. Gaupp, J.M. Hancock, L. Groenendaal and J.R. Reynolds, *Adv. Funct. Mater*., 2003, **13**, 541.

17 J. Foroughi, G. M. Spinks, G. G. Wallace, and . Philip G. Whitten, *Synth. Met*., 2008, **158**, 104.

18 J. M. Jiang, W. Pan, Sh.L Yang and G. Li, *Synth. Met*., 2005, **149**, 181.

19 H. Okuzaki, M. Ishihara, *Macromol. Rapid Commun*., 2003, **24**, 261.

20 Y. Liu, X. Li, J. Ch. Lü, *J. Appl. Polym. Sci*., 2013, **130**, 370.

21 Sh. L. Cui, Z. Q. Zhao and W. Sh. Wei. *J. Appl. Polym. Sci*., 1999, **72**, 1039.

22 Y. Xia, Y. Lu. *Polym. Compos*. 2010, **31**, 340.

23 T. Takahashi, M. Ishihara and H. Okuzaki, *Synth. Met*., 2005, **152**, 73.

24 N. Toptaş, M. Karakışla and M. Saçak, *Polym. Compos*., 2009, **30**, 1618.

25 Y. T. Xu, X. Li, X. N. Li, R. Wang and Zh. K. Yang, *Acta Mater. Compos. Sinica*., 2012, **29**, 111.

26 R. G. Jin, Y. Q. Hua. Polymer Physics, Beijing: Chemical Industry Press, 2006, p 176.

